The phase diagram of QCD at small chemical potentials

Sourendu Gupta*
Department of Theoretical Physics,
Tata Institute of Fundamental Research,
Homi Bhabha Road, Mumbai 400005, India.

We investigate the phase diagram of QCD at small chemical potentials, *i. e.*, when chiral and flavour symmetry breaking involves the pairing of a quark and an antiquark. The phase diagram of two-flavour QCD at small chemical potentials involves chiral symmetry restoration and charged pion condensation. We extend previous studies of the topology of the phase diagram, in sections with high degree of symmetry, to the physical case of fully broken flavour symmetry, using generic thermodynamic arguments. We argue that the extension is unique and present the result. In three flavour QCD the phase diagram for chiral symmetry restoration is less well constrained. However, we argue that present lattice data allows just two different phase diagrams, which we discuss.

PACS numbers:

I. INTRODUCTION

More than thirty years after the first discussions about a phase transition in QCD [1], only small portions of the phase diagram have been explored. Although the complete phase diagram of QCD is of high dimensionality, experiments can at best explore a three dimensional section of the full phase diagram. Further, collisions of heavy-ions have only a single control parameter, the CM energy, $\sqrt{S}$. As a result they explore a single line in this three-dimensional phase diagram. By varying the nuclei being collided, one could, perhaps, extend the search to a small patch around the line. The field is wide open for new ideas on experimental coverage of the QCD phase diagram.

Theoretical work is no less constrained by the tools of the trade. In regions of high symmetry (for example, when the quark masses vanish), universality arguments [2] have been used to put constraints on the phase diagram. Such arguments are realized in models, for example, effective meson models, four-Fermi models or random matrix models, which have the same symmetries as QCD. The resulting predictions of universal properties, *e. g.*, the order of the transition and critical indices, are expected to coincide with QCD. Since the locations of phase transitions are not universal, models should be used to constrain the topology of the phase diagram rather than quantitative predictions of the location of phase boundaries or critical points. When the symmetries are broken, as in the real world, the usefulness of these models is curtailed further. Weak coupling methods for QCD give precise quantitative predictions, but for high temperatures and densities, when the QCD coupling is small enough. Lattice computations were long confined to the region with vanishing chemical potentials, extensions to finite chemical potential being constrained by the fermion-sign problem. The first systematic non-perturbative treatments of QCD at non-vanishing chemical potential using lattice methods have now begun, and the first results are now available [3]. In spite of these limitations, tremendous progress has been made. As we demonstrate in this paper, known results can now be uniquely exended, using only thermodynamic arguments, to yield the topology of the full phase diagram of two flavour QCD and strongly constrain it for three flavours.

The topology of the phase diagram of QCD is constrained by its symmetries. It is well-known that QCD possesses a set of approximate global symmetries, called flavour symmetries, related to the phases of quark wavefunctions. QCD with two flavours of massless quarks would possesses a chiral symmetry $SU_L(2) \times SU_R(2)$ (L and R are transformations on left and right handed quarks respectively). The up and down quark masses (m_u, m_d respectively) break this symmetry. Since $m = (m_u + m_d)/2$ is non-zero the chiral symmetry is broken to the diagonal vector symmetry, $SU_V(2)$, called isospin. Since m is of the order of a few MeV, and much smaller than the scale, Λ_{QCD}, chiral symmetry is approximately valid, being broken at the level of 5–10%. The mass difference $\Delta m = m_d - m_u$ is non-zero but small, thus violating isospin symmetry by a small amount. There is also a semi-light quark flavour, the strange, which has mass, m_s, comparable to Λ_{QCD}. Including this extends the chiral group to $SU_L(3) \times SU_R(3)$ [4]. According to data, this symmetry is broken at the 25% level down to the two-flavour symmetry $SU_L(2) \times SU_R(2)$ [5]. In addition to these approximate flavour symmetries there is also the exact phase symmetry $U_B(1)$ whose charge is the baryon number. The axial phase symmetry, $U_A(1)$, is broken at $T = 0$ by instantons. There is mounting evidence

*Electronic address: sgupta@tifr.res.in

that this symmetry is not restored through a phase transition [6]. In this paper we shall assume that there is no $U_A(1)$ restoring phase transition in QCD.

The large global symmetries of QCD can be broken in many ways, thus giving rise to a complicated phase diagram. In this paper we confine ourselves to the phase diagram at small chemical potentials. By this we mean that the order parameters involve pairing of quarks and antiquarks. At larger chemical potentials there are other interesting phases where the pairing could be between two quarks [7]. We do not examine these phases in this work. A range of intermediate chemical potentials may exist where both quark-antiquark and quark-quark pairings need to be taken into account [8]. If this is so, then some details of the phase diagrams presented here would have to be extended.

Since the phase diagram is structured around the breaking of chiral and flavour symmetry, one might expect that it is independent of the number of colours, N_c. This is correct for $N_c \geq 3$. For the specific case of $N_c = 2$, however, the fact that quark representations are real means that the chiral symmetry is enhanced. As a result, the considerations below do not apply to $N_c = 2$. There is a large body of literature on this particular case, and we refer the interested reader to a recent review [9]. Interestingly enough, as $N_c \to \infty$ the fact that a baryon contains N_c quarks implies that the region of small chemical potentials, in the technical sense adopted here, increases to $\mu \propto N_c$. As a result, several interesting new phases open up in the hadronic regime and may be studied using different order parameters [10].

We argue here that thermodynamic considerations allow us to extend presently available knowledge to large parts of the parameter space of QCD and enable us to build a qualitative picture of the complete phase diagram of QCD for small chemical potential. We deduce the topology of the three dimensional slice of the phase diagram of two-flavour QCD which may be accessible to experimental tests. We also indicate how these arguments allow us to constrain the phase diagram of QCD with up, down and strange quarks.

The plan of this paper is the following: in the next section we briefly review the Gibbs' phase rule in the form that we will use it. The two sections following that deal with $N_f = 2$ and 3 respectively. The final section contains a summary of our results.

II. THE GIBBS' PHASE RULE

In this paper we investigate the phase diagram of QCD using an essential tool of thermodynamics: the Gibbs' phase rule. Before stating the rule we recall that a system in thermodynamic equilibrium is fully described by a certain number of extensive thermodynamic quantities. This set of extensive quantities, among which we must always count the entropy S and the energy E, serve as coordinates in the so-called Gibbs space. The thermodynamically stable states of a system are in one-to-one correspondence to a convex surface $E(S, \cdots)$ in Gibbs space. The thermodynamic intensive quantities are derivatives of E with respect to one of the other extensive quantities, the derivative with respect to S being T. By the process of taking Legendre transforms of E with respect to each of the intensive variables, one reaches a description of thermodynamics in terms of the intensive quantities and a free energy, $\mathcal{G}$, which is extensive. A phase diagram is obtained by projecting out information on $\mathcal{G}$, and describes the regions in which different phases of a system are thermodynamically stable.

By construction almost all points in the phase diagram correspond to one pure phase. This is the one with the lowest free energy among all possible phases. If the system has more than one phase, then at some points in the phase diagram two phases may coexist. If we label the phases by a and b, then the condition for coexistence is the equality of free energy densities in the two phases,

$$g_a(T, \mu_u, m_u, \cdots) = g_b(T, \mu_u, m_u, \cdots), \tag{1}$$

If the dimension of the phase diagram is D, then two phases coexist along solutions of the above equation, *i. e.*, generically along hypersurfaces of $D-1$ dimensions. Three-phase coexistence requires simultaneous equality of three free energies, and hence occurs along hypersurfaces of $D-2$ dimensions. This surface of 3-phase coexistence is clearly the intersection of three surfaces of 2-phase coexistence, obtained by taking the phases pairwise. $\mathcal{P}$ phases generically coexist along hypersurfaces of $D+1-\mathcal{P}$ dimensions, which are the intersection of $\mathcal{P}$ surfaces of two-phase coexistence. This is one form of the statement of Gibbs' phase rule.

A two-phase coexistence surface either has no boundary or ends in a surface of one lower dimension, $D-2$, called a critical surface. Similarly, a 3-phase coexistence surface may have a boundary. Such a boundary is a $D-3$ dimensional surface called a tricritical surface. Since the 3-phase coexistence surface is the intersection of three 2-phase coexistence surfaces, the tricritical surface is the intersection of three critical surfaces [11]. Boundaries of $\mathcal{P}$-phase coexistence surfaces, when they exist, are called $\mathcal{P}$-critical surfaces, and can be viewed as intersections of $\mathcal{P}$-critical surfaces. Clearly a $\mathcal{P}$-critical surface is one at which $\mathcal{P}$ different phases simultaneously become indistinguishable. Thus another form of Gibbs' phase rule states that when the dimension of the phase diagram is D, then there may be $D-1$ dimensional surfaces of two-phase coexistence (first order phase transitions), $D-2$ dimensional critical surfaces, $D-3$ dimensional tricritical surfaces, *etc.*.

The most well-known application of the rule is to phase diagrams of chemically pure substances (for example, water), characterised by two intensive parameters T and the pressure P. Since $D = 2$, one has lines of two-phase coexistence. Such lines can either end in critical points, or two such lines can meet at isolated triple points (*i. e.*, points of three phase coexistence). Both these possibilities are realized in the well-known phase diagram of water. A different example is in mixtures of two chemically pure substances (water-alcohol, binary alloys, QCD with quarks, *etc.*), where an additional intensive parameter, the chemical potential μ, makes the phase diagram three dimensional. In this case one has surfaces of two-phase coexistence, bounded by critical lines. Three surfaces can intersect along lines of three-phase coexistence. The end point of such a line is a tricritical point, and one can view this point also as the crossing point of three critical lines. The realization of these possibilities in He^3-He^4 mixtures was treated in [11].

If the phase diagram is known only in some part of the space of intensive variables where calculations are tractable, then the Gibbs' phase rule allows us to constrain the possibilities that arise from extrapolations to larger parts of the space. As we show in the coming sections, the constraints are enormous, and sometimes they determine the topology of the phase diagram completely.

In QCD a choice of the extensive quantities can be the order parameters for the breaking of chiral symmetry (one condensate for each flavour of quarks and the net number of quarks of each flavour). Conjugate to these are the couplings— the quark masses and the chemical potentials respectively. Adding to this set the total energy, one sees that for $N_f = 2$ the phase diagram has 5 dimensions. For $N_f = 3$ the strange quark mass and chemical potential are added, as a result of which the phase diagram is 7 dimensional. Experiments are constrained to work with given quark masses, and hence explore a phase diagram of dimension 3 for $N_f = 2$ and dimension 4 for three flavours.

This is true if one examines a strongly interacting system on a time scale much larger than the slowest strong interaction related relaxation time, but much smaller than the time scale of the flavour changing weak interactions. This is the case in heavy-ion collisions, where the expanding fireball cools and freezes out on time scales of the order of a few fermis, whereas the typical strangeness changing time scale is many orders of magnitude larger. This might seem to indicate that the full 4 dimensional phase diagram can be explored. However, in the initial state the only conserved quantum numbers are the baryon number, B, and the electrical charge, Q. Since these two, and the total energy, are the only quantities which can be manipulated in experiments, the three dimensional slice of the phase diagram conjugate to these variables is the only part of the full phase diagram which is accessible to any possible experiment. As is well-known, other parts of the $N_f = 3$ phase diagram may become accessible in situations at high densities and relatively low temperatures, where Fermi-blocking of the light quark states may increase the lifetime of strange quarks. This situation may well be realized in compact stellar objects. In the early universe, around the time of the QCD phase transition, the baryon density is much higher than now, but still small enough that $\mu_B \ll T$. Also, the inverse Hubble time is much smaller than it is now, but much larger than weak the weak interaction time scale. Hence, in the early universe, both strong and weak interactions should be considered to be in equilibrium, so that the phase diagram reverts to being 3 dimensional. Unfortunately, the chemical potentials in the early universe are so small that essentially only the temperature axis is explored.

III. TWO FLAVOURS

For $N_f = 2$ QCD the five intensive quantities can be chosen to be T, μ_u, μ_d, m_u and m_d. A common alternative choice is to use μ_B, conjugate to the baryon number, B, and μ_I, conjugate to the third component of isospin, I_3. Moving between the ensembles corresponding to these is straightforward; detailed formulae are given in [12]. It is useful to note that these intensive quantities are conjugate to the extensive thermodynamic variables

$$N_u = \frac{\partial \mathcal{G}}{\partial \mu_u}, \qquad \mathbf{s}_u = \frac{\partial \mathcal{G}}{\partial m_u}, \tag{2}$$

and similar relations for down quarks, where N_u is the net number of up quarks and $\mathbf{s}_u$ is an extensive quantity whose density is the up quark condensate $\langle \overline{u} u \rangle$.

A. Finite temperature

The best-known part of the phase diagram for $N_f = 2$ QCD is the temperature axis for $m = \Delta m = \mu_B = \mu_I = 0$ [2]. The action has the chiral symmetry $SU_L(2) \times SU_R(2)$. At $T = 0$ this is spontaneously broken to the isospin part, $SU_V(2)$, resulting in three massless pions arising as the Goldstone bosons of the broken symmetry. In the high temperature limit the symmetry is restored. The symmetry of the theory is isomorphic to O(4), which is known to have a second order phase transition. Universality then indicates that there is a critical temperature, T_c, at which a second order phase transition occurs from the chiral symmetry broken phase to the symmetric phase with critical

exponents in the O(4) symmetry class. The order parameter is the isoscalar chiral condensate, $\mathbf{s} = (\mathbf{s}_u + \mathbf{s}_d)/2$, which changes from a non-zero value at low temperatures to zero at T_c. For $T < T_c$ the order parameter is negative for any positive m, and flips sign when m in negative. Hence there is a line of first order phase transitions for $m = 0$ and $T < T_c$, which ends in the critical point at T_c. There is no finite temperature phase transition at finite m.

Lattice computations are performed at finite quark mass, and are consistent with this picture since they observe only a cross over [32]. Chiral extrapolations have given mixed results: there is no agreement on the critical exponents which are seen. This could be a finite lattice spacing artifact. Several studies have used staggered quarks which, for $m = 0$, have only an $U(1) \times U(1)$ chiral symmetry at finite lattice spacing. The chiral transition in this case should lie in the $O(2)$ universality class. It turns out to be hard to distinguish O(4) and O(2) exponents [14]. Lattice studies are consistent with both [15]. Studies with Wilson quarks show results consistent with critical exponents in the $O(4)$ universality class [16]. The situation can be clinched in simulations with dynamical overlap quarks, which realize the full chiral symmetry. However, these simulations are currently in their infancy.

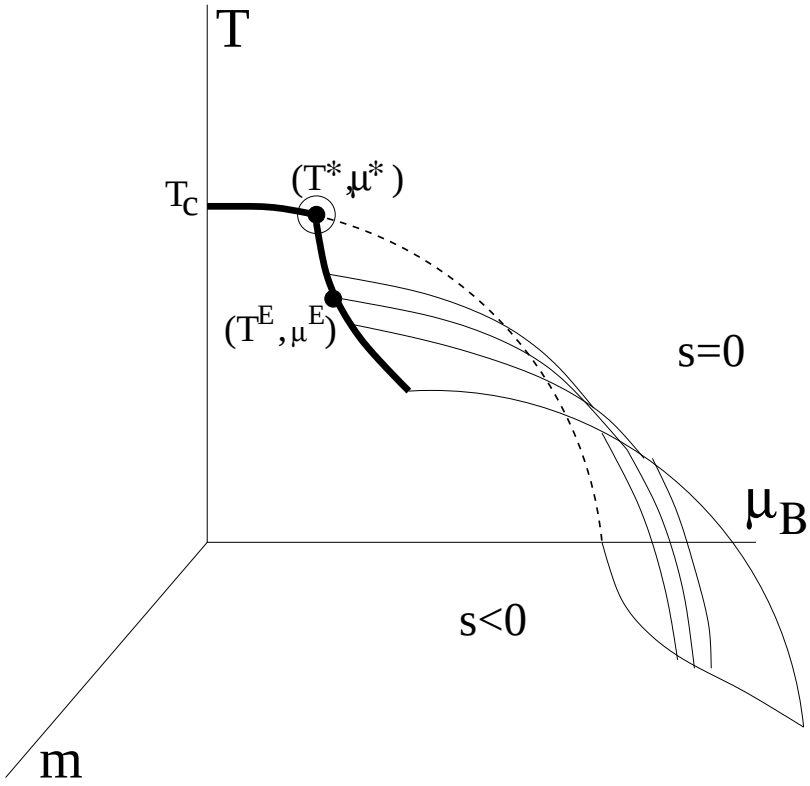

FIG. 1: The phase diagram in the T-μ_B-m space [17] (only the side for $m \geq 0$ is shown; a symmetric part of the figure for $m \leq 0$ is obtained by switching the sign of the order parameter $\mathbf{s}$). A critical line in the $O(4)$ universality class starts from the chiral phase transition, T_c and is the boundary of the first order surface separating the phases with opposite signs of $\mathbf{s}$. The tricritical point at (T^*, μ^*) for $m = 0$ lies at the end of the triple line (dashed curve). At the physical quark mass one expects a critical end point, (T^E, μ^E), in the Ising universality class. This lies on the critical line which is the boundary of the first order surface separating the phases with non-vanishing and zero value of the order parameter.

B. The T-μ_B-m section with and without isospin symmetry

Recently attention has been focused on the three dimensional section of the phase diagram with varying T, μ_B and m and fixed $\Delta m = \mu_I = 0$. Using the order parameter $\mathbf{s}$ one finds the phase diagram shown in Figure 1. The plane $\mu_B = 0$ was described in the previous subsection. The first order line and its O(4) critical end point described there extends naturally to three dimensions, becoming a surface of 2-phase coexistence (corresponding to a sign flip in $\mathbf{s}$) with a critical line as boundary in the $m = 0$ plane. For positive m there is a 2-phase coexistence surface across which a large negative value of $\mathbf{s}$ changes discontinuously to a smaller value. For $m < 0$ there is a symmetrically placed coexistence surface with the sign of $\mathbf{s}$ reversed. These three 2-phase coexistence surfaces intersect in a triple

line in the $m = 0$ plane. Since there is a critical line bounding one of these surfaces, it must meet the triple line at a tricritical point. We are led to the conclusion that all three 2-phase coexistence surfaces are bounded by critical lines, and the tricritical point, at (T^*, μ_B^*), is their common intersection point.

One fact about this phase diagram is worth emphasizing. The quantity $\mathbf{s}$ is an order parameter related to symmetry only on the $m = 0$ plane in Figure 1, since it is exactly zero everywhere above the triple-phase and critical lines. At finite m, above the coexistence surface it is not exactly zero, but has a value proportional to m. Below this surface it has a much larger value. Across the coexistence surface it has a discontinuity, and hence can be used to flag a first order phase transition even at finite m. However, along the wing critical lines, $\mathbf{s}$ is not an order parameter in the sense of being zero in one phase and non-zero in another. This is related to the fact that, for $m \neq 0$, the phase transition is not related to a symmetry. However, along the critical line there are long range correlations between local fluctuations in $\mathbf{s}$, or, equivalently, through a fluctuation-dissipation theorem, there are divergent susceptibilities of $\mathbf{s}$. This kind of critical behaviour is said to be a liquid-gas transition, and expected to be in the Ising universality class.

The slopes of the coexistence surface can be determined by a generalization of the Clapeyron-Clausius equations. For the case at hand we can write

$$d\mathcal{G}_i = S_i dT + B_i d\mu_B + \mathbf{s}_i dm, \tag{3}$$

where the subscript i refers to the two phases (say, a and b) which are at equilibrium along the coexistence surface. As one moves along the surface, the changes dT, $d\mu_B$ and dm are related by the fact that the free energy density is the same in the two phases, eq. (1). In order to define a density in a relativistic theory, one notes that all four extensive quantities scale similarly, and hence any one of them can be used as a normalization. In determining the slope of the coexistence surface, one has to hold one of the three intensive quantities fixed, so one can choose to use the extensive quantity conjugate to it to perform the normalization.

Along lines of constant m, one can then normalize all extensive quantities by $\mathbf{s}$ to get the relation

$$\left.\frac{d\mu_B}{dT}\right|_m = -\frac{1}{B}\,\frac{S_a/\mathbf{s}_a - S_b/\mathbf{s}_b}{1/\mathbf{s}_a - 1/\mathbf{s}_b}. \tag{4}$$

Since the right hand side is independent of the sign of the chiral condensate, one can use the magnitude $|\mathbf{s}_{a,b}|$ in the expression. Choose a to be the low temperature phase and b to be the high temperature phase. Then, as is shown by lattice computations, $S_a < S_b$ and $|\mathbf{s}_a| > |\mathbf{s}_b|$. As a result, the expression on the right is negative, implying that with increasing T the surface of coexistence moves to smaller μ, as shown in Figure 1.

Since the ordering of the entropy and chiral condensate determine the slope, the figure is consistent with the idea that the low temperature phase contains hadrons, whereas the high temperature phase contains quarks [12]. At finite m one then has a line of first order transitions starting at $T = 0$ and a large μ_B and ending in a critical end point at (T^E, μ_B^E) which is in the Ising universality class. These arguments, based on the Gibbs' phase rule and the Clapeyron-Clausius equation, reproduce the results of earlier model studies [17], which spurred recent developments in lattice QCD [3] and gave rise to experimental interest in the search for the QCD critical point [18].

One can extend such arguments to the other two slopes. Along lines of constant μ_B one finds

$$\left.\frac{dT}{dm}\right|_{\mu_B} = \frac{|\mathbf{s}_a| - |\mathbf{s}_b|}{S_a - S_b}. \tag{5}$$

Given the relative magnitudes of the entropies and chiral condensates, one finds that this slope is negative, *i. e.*, at constant μ_B, the temperature of coexistence decreases with increasing quark mass. Along lines of constant T one finds the slope

$$\left.\frac{d\mu_B}{dm}\right|_T = -\frac{1}{B}\,\frac{|\mathbf{s}_a|/S_a - |\mathbf{s}_b|/S_b}{1/S_a - 1/S_b}, \tag{6}$$

which is positive. To the best of our knowledge, arguments about these slopes based on the Clapeyron-Clausius equations are new. They imply that with increasing quark mass the critical end point, (T^E, μ_B^E), moves to larger T and smaller μ_B, as indicated by current lattice data [19].

C. The section T-μ_B-μ_I when $\Delta m = 0$

The three-dimensional slice through the $N_f = 2$ phase diagram which is obtained for a fixed non-vanishing value of m and $\Delta m = 0$ (including the special slice which also has $\mu_B = 0$) has been extensively examined in the literature

[20, 21, 22]. This case has one very attractive feature: the quark determinant is positive definite, and hence lattice simulations are possible, and they can be used to check arguments using global symmetries. The drawback is that the symmetry which makes the quark determinant positive definite is responsible for making the phase diagram non-generic.

The plane of T-μ_I, for arbitrary m and vanishing μ_B and Δm,was first discussed in [20]. Using an effective theory, it was argued that along the line $T = 0$, there should be a phase transition which results in the development of a charged pion condensate, $\mathbf{p} = \overline{\psi}\gamma_5\tau_1\psi$. It was argued that the phase transition should be critical and in the $O(4)$ universality class with critical $\mu_I^c = m_\pi$, and that an $O(2)$ critical line emanate from it. Now, the Gibbs phase rule does not generically allow a critical line in a two-dimensional phase diagram. However, subsequent lattice computations [21] saw instead a first order line at finite T connecting to a critical or tricritical point with $\mu_I^c \propto m_\pi$.

The phase diagram was extended to the three dimensional slice T-μ_B-μ_I for finite m and $\Delta m = 0$ by three different methods in [22]. In all these works, critical lines were obtained in the μ_I-μ_B surfaces for generic T. Thus there are critical surfaces in this three dimensional phase diagram. Such a violation of the Gibbs phase rule may occur in subspaces of high symmetry. For example, in the plane $m = \Delta m = \mu_I = 0$, one found the O(4) critical line shown in Figure 1. However, these exceptions are non-generic; when extending the phase diagram they do not develop into higher dimensional surfaces. This is clear in the above example. In the same way, one is forced to the conclusion that the slice $\Delta m = 0$ is not generic. We consider extensions to $\Delta m \neq 0$ next.

D. Isospin broken by quark masses

1. *The phase diagram in T-μ_I-Δm*

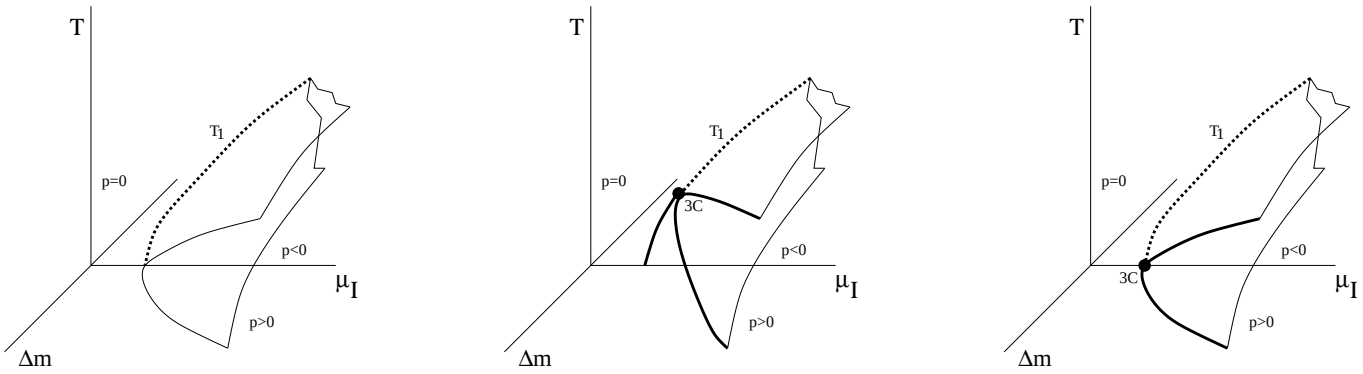

FIG. 2: The phase diagram in the T-μ_I-Δm space for generic non-zero m and $\mu_B = 0$. Since there is a two phase coexistence surface on the plane $\Delta m = 0$ which separates phases with opposite signs of p, this plane also contains a line of triple-phase coexistence (dashed, marked T_1). This line may (second and third panels) or may not (first panel) end in a tricritical point at $T = 0$. The last phase diagram is favoured, as we discuss in the text.

Once isospin is broken by a mass difference between the up and down quarks, an isospin chemical potential no longer matches the up quark and down antiquark Fermi surfaces exactly. This breaks the symmetry that kept the full quark determinant non-negative, and hence presents the usual problems for lattice simulations. However, it gives a generic phase diagram in T-μ_I.

Consider the section of the phase diagram for generic non-zero m and $\mu_B = 0$. Changing the sign of Δm is equivalent to toggling the definition of u and d flavours (in the absence of electroweak interactions) and hence to flipping the sign of μ_I. Thus, if there is charged pion condensation, *i. e.*, $|\mathbf{p}| > 0$, for some value of μ_I, then there is a first order transition across $\Delta m = 0$, in which the sign of p distinguishes the two phases. Thus, along some line in the $\Delta m = 0$ plane one expects triple-phase coexistence, the phases corresponding to $\mathbf{p} = 0$ and two non-zero values of $\mathbf{p}$ of opposite sign.

As one goes from small to large μ_I along a line of fixed Δm and T, the order parameter $\mathbf{p}$ increases. Hence, by adapting the argument based on the Clausius-Clapeyron equations for the T-μ_B-m phase diagram, one obtains the slope drawn in Figure 2. Such a 3-phase coexistence line can be accommodated by the three possible phase diagrams shown in Figure 2.

The first possibility shown in the figure is generic. The triple-phase line, T_1, starts at $T = 0$ and continues up. There is no critical boundary to the three surfaces of first order transitions. This phase diagram is ruled out by the

results of [20, 21] which point to some kind of criticality at $T = \Delta m = 0$. However, the $SU_V(2)$ isospin symmetry is broken to a vector U(1) when $\Delta m \neq 0$. As a result, an O(4) critical point is not stable under this perturbation.

The second generic possibility shown in Figure 2 takes this fact into account. The triple-phase line, T_1, ends at a tricritical point. Three critical lines emerge from this point. One lies in the symmetry plane $\Delta m = 0$ and at $T = 0$ it is seen to be the O(4) critical point identified in [20]. Along the two wing critical lines the remnant vector $U(1)$ symmetry is broken by charged pion condensation. This is closely analogous to the phase diagram in Figure 1. In this scenario, as one traverses a line of fixed $\Delta m \neq 0$ for $T = 0$ by varying μ_I, one should go continuously from a phase with small $\mathbf{p}$ to one with a large value of this condensate. However, at $T = 0$ and small μ_I it is not energetically feasible for pions to condense, hence there must be a range of μ_I over which $\mathbf{p}$ vanishes. In that case a phase transition must occur at $T = 0$ for any μ_I.

This brings us to the final possibility: the triple-phase line ends at $T = 0$ in a tricritical point. Two wing critical lines emerge from this in the $T = 0$ plane. The third critical line, which is the O(4) line of the second scenario, is squashed down to a point. In this scenario there is always a phase transition between the charged pion condensed and uncondensed phases. This is the favoured phase diagram, since the lattice computation of [21], which sees a critical or tricritical point at $T = 0$ and $\Delta m = 0$, prefers this over the first scenario. It would be good to check this through another computation at smaller lattice spacing.

2. *The T-μ_B-Δm phase diagram*

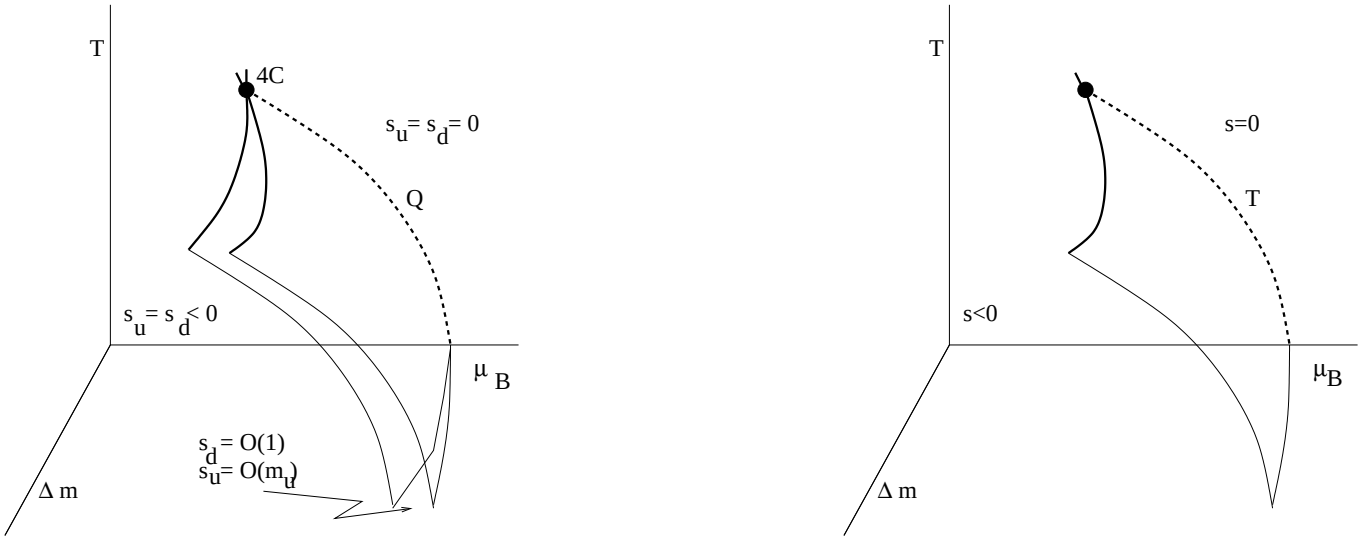

FIG. 3: Two possible topologies for the phase diagram in T-μ_B-Δm for $\mu_I = 0$. The second one is preferred (see the text for details).

One might expect that when the isospin symmetry is broken, the flavour singlet order parameter should be replaced by the pair $\mathbf{s}_u$ and $\mathbf{s}_d$ [22]. If so, the T-μ_B phase diagram would be extended to the first topology shown in Figure 3. This contains a line of 4-phase coexistence, labeled Q in the diagram with an end point which is a tetracritical point. In a three dimensional phase diagram one does not generically expect either a 4-phase coexistence line or a tetracritical point. We have argued before that non-generic situations might be obtained on sections of high symmetry. However, having two different non-vanishing masses breaks the flavour symmetry maximally, so it is impossible to find a more generic situation.

This no-go argument can be evaded by noting that μ_I and Δm break the flavour symmetry to the same subgroup. As a result, it is possible that the topology is the same in the two sections T-μ_B-Δm for $\mu_I = 0$ and T-μ_B-μ_I for $\Delta m = 0$ separately. In other words, the 4-phase coexistence line and the tetracritical point lie in the intersection of these two sections in this extended four dimensional phase diagram T-μ_B-μ_I-Δm. By the same token, such a topology is ruled out as non-generic in the T-μ_B-μ_I section for $\Delta m = 0$ unless it is also seen in this section.

Arguing differently, one might expect that for $\Delta m/m < 1$ the effect of isospin symmetry breaking through the quark masses should not change the phase diagram qualitatively. In that case the two order parameters $\mathbf{s}_u$ and $\mathbf{s}_d$

would be redundant, and the two sheets of first order transitions merge into a single sheet of first order transitions found with **s**. This possibility is shown as the second topology in Figure 3.

If this second argument is correct, then one must face the question of what happens at large $\Delta m/m$. Exactly this question was answered at $T = 0$ using an effective theory in [23]. At finite Δm, the explicit breaking of isospin symmetry to vector U(1) allows the π^0 to mix with isoscalars (this allows a change in its mass without changing the masses of $\pi^{\pm}$). When $\Delta m/m$ is large, a neutral pion condensate can form, and, at $T = 0$, there is a second order transition between phases with and without this condensate. In the real world a mass difference between the charged and neutral pions is observed, so a mixing of this sort could occur. However, a neutral-pion condensate is not observed at $T = 0$, so one may conclude that the physical value of $\Delta m/m$ is not large enough for isospin breaking effects to qualitatively change the phase diagram shown in the second part of Figure 3.

The mixing of neutral pions with isoscalars is a physical effect which does not exist in the models used in [22]. This leads us to prefer the second phase diagram shown in Figure 3. The only lattice study to date of thermodynamics at finite Δm [24] saw no evidence of two separate crossovers. A computation with a different lattice formulation of quarks will be an interesting and useful additional piece of evidence.

E. The physical phase diagram

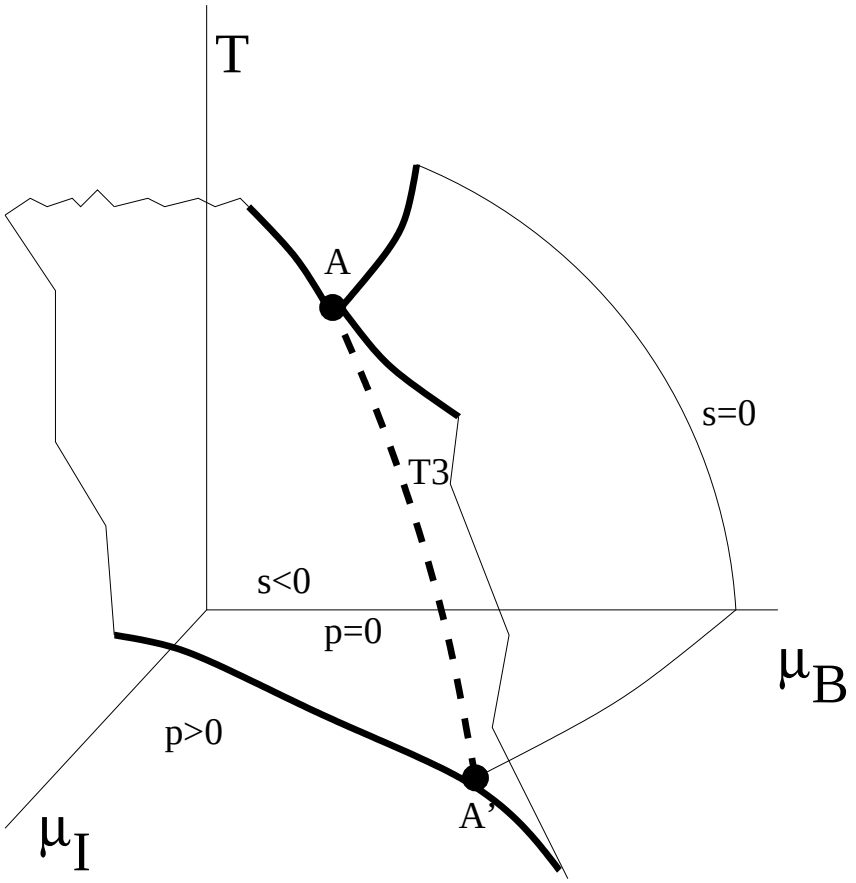

FIG. 4: The phase diagram in the T-μ_B-μ_I space for generic non-zero m and Δm is organized by the two order parameters **s** and **p**. It contains a line of 3-phase coexistence (labeled $T3$) and two tricritical points (labeled A and A').

The physical phase diagram of QCD is the one in which all possible experimentally tunable parameters are shown for fixed physical values of the remaining parameters. This is the phase diagram in the space of T-μ_B-μ_I for generic small m and $\Delta m < m$. After the analysis of the previous subsections, deducing the topology of this phase diagram is straightforward. The various phases are distinguished by the order parameters **s** and **p**. We discuss the topology of the phase diagram (shown in Figure 4) only in the quadrant with $\mu_{B,I} > 0$. The remainder can be constructed by symmetry.

In the $\mu_I = 0$ plane there is a first order line ending in the QCD critical point. Across this line $\mathbf{s}$ changes discontinuously. Following the discussion of the previous subsection, we conclude that this line develops into a surface of 2-phase coexistence. The QCD critical end point develops into a critical line (in the liquid-gas universality class) which is the boundary of this surface. In the $\mu_B = 0$ plane there is a first order line separating phases with vanishing and finite values of $\mathbf{p}$ with a liquid-gas critical point at $T = 0$. This develops into a 2-phase coexistence surface.

The two first order surfaces must meet along some line, $T3$. Hence $T3$ is a line of 3-phase coexistence, and another surface of 2-phase coexistence must emanate from it, separating the phase in which both the condensates vanish from that in which neither does. The two ends of $T3$, labeled A and A', must both be tricritical points. At A the first order surface of discontinuity in $\mathbf{p}$ must have a boundary. Since the system has no particular symmetry at A, all three critical lines meeting at this point must be in the universality class of a liquid-gas transition. At A' there seem to be two critical lines, both in the liquid-gas universality class. The third critical line is degenerate, as in the third topology shown in Figure 2.

The derivation of the Clapeyron-Clausius equations for the physical phase diagram needs little further comment. Along planes of constant μ_B one can use eq. (4), since m and Δm are also constant along this line. Along the planes where μ_I are constant, the modification of eq. (4) was already discussed in Section III D 1, and leads to the opposite slope of the coexistence surface for pion condensation. The remaining part involves scaling the expression $d\mathcal{G}_i = S_i dT + B d\mu_B + I_3 d\mu_I$ by S_i in the phase i, and equating the two free energy densities so defined at each coexistence surface. The resulting Clapeyron-Clausius equation is

$$\left.\frac{d\mu_B}{d\mu_I}\right|_T = -\frac{I_3}{B}. \tag{7}$$

The first order surface of chiral symmetry restoration, which is in the phase without a pion condensate, then has only weak dependence on μ_I. Similarly, the first order surface of pion condensation has weak dependence on μ_B because the baryon density is low in the phase with chiral symmetry breaking. The surface separating the phase with both condensates vanishing from the phase where both condensates are present has more complicated behaviour. One expects that in the phase without condensates the number densities scale with chemical potentials as $B \propto \mu_B^3$ and $I_3 \propto \mu_I^3$ when T is small. In that case this first order surface is roughly linear in μ_B and μ_I. Lattice computations at $\Delta m = 0$ can substantially improve our knowledge of the functional form of $B(T, \mu_B, \mu_I)$ and $I_3(T, \mu_B, \mu_I)$, and therefore the shape of the physical phase diagram through continuation to $\Delta m \neq 0$.

The position of A and A' are constrained by these considerations. It is estimated that the QCD critical end point at $\Delta m = \mu_I = 0$ is at $\mu_B^E/T^E \simeq 1$ with $T^E \simeq 170$–190 MeV. Since the effect of isospin breaking is small, one expects that at realistic values of Δm the critical end point does not shift drastically. One also knows that at $\mu_B = \Delta m = 0$, the critical point in $\mu_I \simeq m_\pi$. The corrections at realistic Δm are not large. One expects that $\mu_B^A \simeq \mu_I^A \simeq T^A \simeq 100$–$200$ MeV. Also, from this topology one could deduce that in heavy-ion collisions where $\mu_I \ll m_\pi$ one should expect to see the QCD critical line close to the estimates of μ_B^E and T^E.

IV. THREE FLAVOUR

For $N_f = 3$ QCD, the intensive quantities at the phase transition are the temperature T, the three quark masses, m_u, m_d and m_s, and the three chemical potentials μ_u, μ_d and μ_s. As before, we can take linear combinations of these variables to parametrize the seven-dimensional phase diagram. We will use the mean light quark mass $m = (m_u + m_d)/2$ and the mass splitting between these two, $\Delta m = m_u - m_d$. It is useful to construct the baryon chemical potential, μ_B and two other combinations, as outlined in [12].

The three flavour phase diagram has barely been explored, and we shall not be able to do justice to the many kinds of pairings that it may possess. In this first work we restrict attention to a question which has been asked recently: is the two-flavour phase diagram for chiral symmetry restoration (Figure 1) a good guide to the corresponding phase diagram in QCD with additional strange quarks?

A. Vanishing chemical potentials

Universality arguments [2] lead us to expect that the chiral phase transition in three flavour QCD at zero chemical potentials is of first order. The order parameter used is the three-flavour condensate. In the three-flavour chiral limit, since the action is blind to flavour, any linear combination of three flavoured condensates is as good an order parameter as any other, so one could as well continue to use the two-flavour order parameter $\mathbf{s}$ to study the phase structure. When the strange quark becomes massive with the light quarks remaining massless, one does not expect

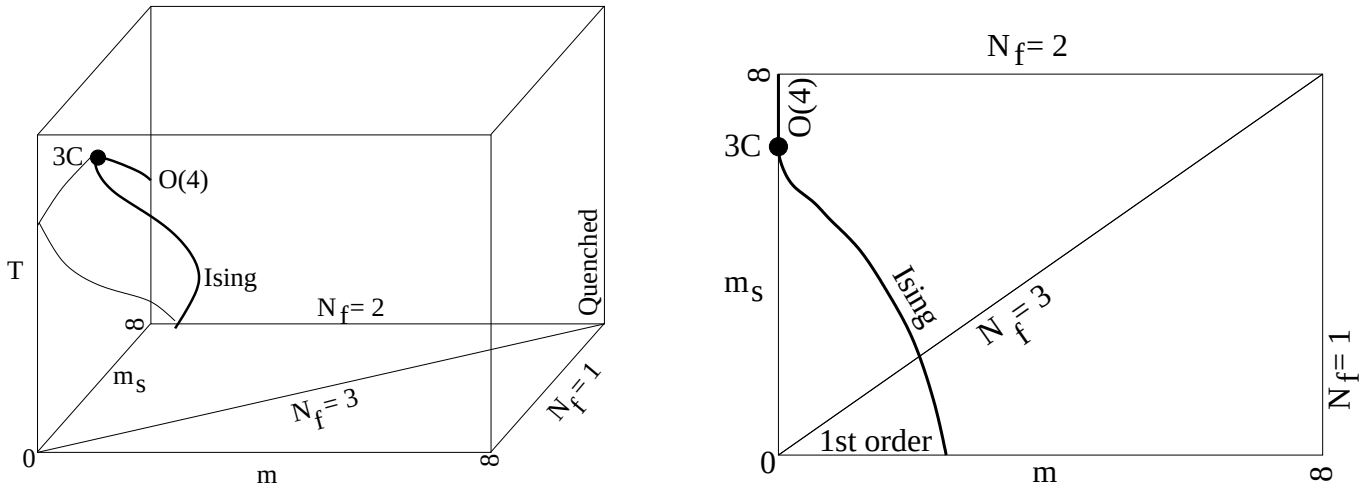

FIG. 5: The phase diagram of QCD for vanishing chemical potentials and $\Delta m = 0$ (on the left) as observed with the light quark condensate. In different parts of this phase diagram different flavour symmetries are obtained: the diagonal plane has exact 3-flavour symmetry, the "back" plane has $N_f = 2$, the far corner is the quenched theory, and the plane at the far right has $N_f = 1$. On the right is the corresponding flag diagram, obtained by projecting the phase diagram to the plane of $T = 0$.

symmetry restoration in the strange sector while the symmetry remains broken in the light quark sector. Similar expectations hold whenever the strange quark mass is heavier than the up and down quark masses. Hence, in this whole region one expects that the same phase structure is seen whether one uses the three flavour condensate or $\mathbf{s}$.

The phase diagram of QCD with three quarks has been explored in several lattice computations [25, 26, 27, 28] where the two light quarks are degenerate, *i. e.*, $\Delta m = 0$. In this case the phase diagram in the section m-m_s-T is of the kind presented in Figure 5. In these studies there is only one chiral phase transition observed, and not separate ones for strange and light flavours, in conformity with the above discussion. For infinite m_s and $m = 0$, one has two flavour chiral symmetry, and hence a second order transition in the O(4) universality class. When $m_s = m$, *i. e.*, three flavour symmetry is exact, one has a line of first order transitions up to a critical end point, which lies in the Ising universality class [27]. Moving off the exact $N_f = 3$ line (termed going to $N_f = 2 + 1$ in the literature), this develops into a surface of first order transitions bounded by a critical line. Since this line is in the liquid-gas universality class [27], it must meet the O(4) line in a tricritical point. The nature of this critical line is crucial in establishing a phase diagram. If it is in the liquid-gas class, as expected, then this would be visible with any formulation of lattice quarks.

The phase diagram shown in Figure 5 can be probed entirely with the light quark condensate. There are, of course, other phase transitions in this phase diagram— for example the deconfining transition in the corner which contains the quenched theory. This is observed with a different order parameter, the Polyakov loop, and hence does not appear in the phase diagram shown.

These results are often presented in a figure (the second of Figure 5) which is the phase diagram projected down to the plane m-m_s. This is not a phase diagram since a point on it does not represent a stable thermodynamic phase. Instead, each point on this diagram represents whether or not there is a phase transition at some T "above" it. Unfortunately there seems to be no name for such an useful diagram, and we are forced to invent a name for it. In the rest of this paper we call it the "flag diagram", because each point flags whether there is a phase transition above it, and if so, the order of the transition.

One of the main open questions about the flag diagram is the location of the physical point. All computations indicate that this lies deep in the crossover region [28, 29]. A second important question is about the location of the tricritical point. What is the value of m_s^{3c}? If the physical strange quark mass is less than m_s^{3c} then the $N_f = 2$ phase diagram will be a good guide to the phase diagram of real QCD. If, on the other hand, the physical strange quark mass is larger, then the phase diagram in the real world could be significantly different. One naively expects that $m_s^{3c} \simeq \Lambda_{QCD}$; since the physical value of m_s is also similar, this is an interesting and wholly non-perturbative question.

One estimate of m_s^{3c} that we are aware of was made using a linear sigma model with parameters fixed by hadronic data [30]. This finds that the K meson mass at the tricritical point is at least 1700 MeV, far in excess of the physical value. While this would seem to indicate that the physical strange quark mass is lighter than m_s^{3c}, there are indications that further work may be needed in order to pin down m_s^{3c}. For example, in [30] it is estimated that the critical end point along the $N_f = 3$ line occurs at $m_\pi^c = m_K^c = 110 \pm 20$ MeV. The lattice computations of [27] indicate that the

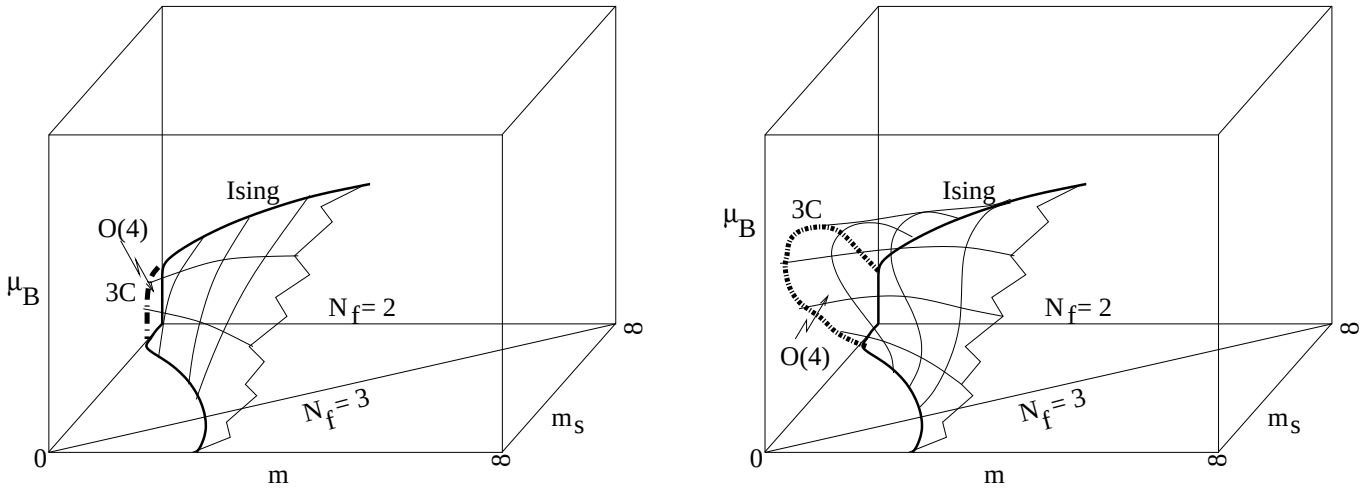

FIG. 6: Possible flag diagrams for three flavour QCD are organized around the shape of the tricritical line (dash-dotted line). The surface of O(4) criticality which lies in the plane with $m = 0$ meets a surface of Ising criticality along this line. The two possibilities shown are distinguished by the approach of the tricritical line to the $\mu_B = 0$ plane. The second possibility includes the case where the tricritical line goes to infinite μ_B somewhere between its two fixed ends.

critical end point may be at $m_\pi^c = m_K^c = 192 \pm 25$ MeV. Whether the discrepancy is due to an insufficiency in the model of [30] or the multiple extrapolations performed in [27], or a combination of the two, remains to be tested in future. In [31] the estimate $m_s^{3c} \simeq 500$ MeV is presented. Indications that the cutoff effects at comparable cutoffs are large come from the results of [28, 29].

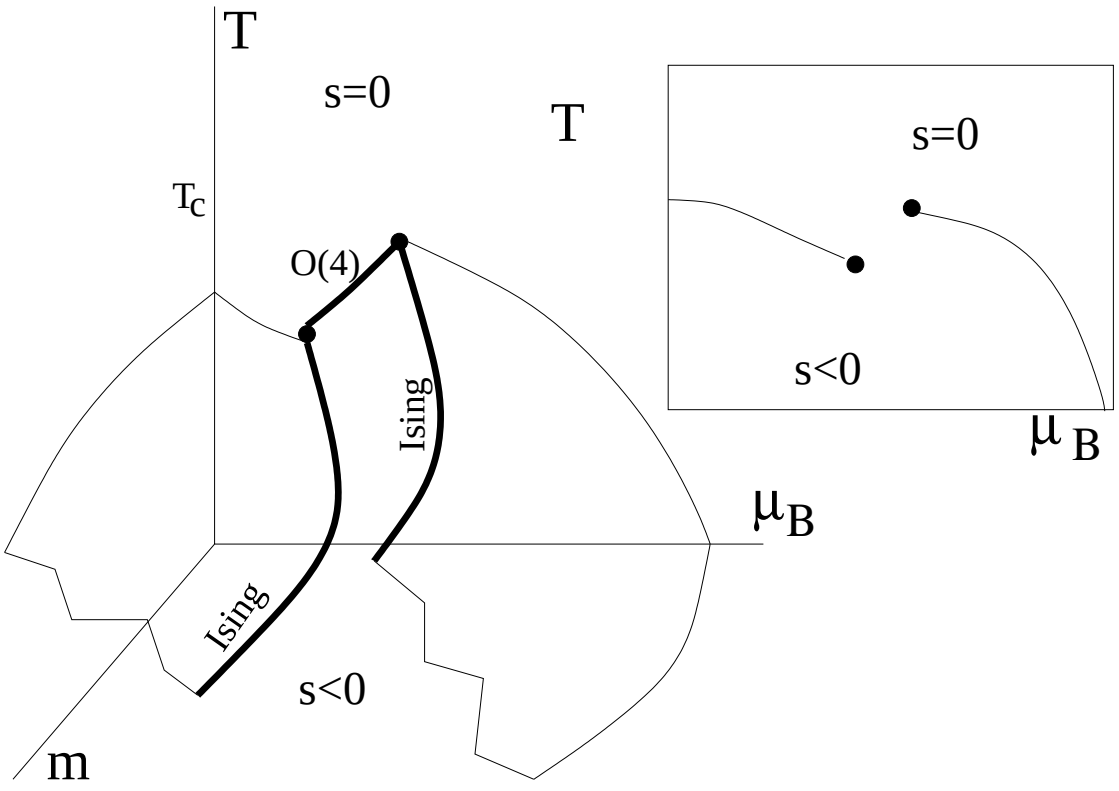

FIG. 7: The phase diagram for fixed $m_s^{turn} < m_s < m_s^{3c}$ and $\Delta m = \mu_I = \mu_Y = 0$ in the second scenario shown in Figure 6. The phase diagram for fixed m is shown in the inset.

B. Finite μ_B

Another slice that is interesting from the point of view of forthcoming planned experiments is the four-dimensional T-μ_B-m-m_s slice obtained with $\Delta m = \mu_I = \mu_Y = 0$. This was investigated recently on the lattice [29, 31], and a flag diagram obtained by projecting out the T axis was used in the presentation. These two studies differ in the conclusions reached: one [29] favours the first flag diagram shown in Figure 6; the other [31], we argue below, is consistent with the second possibility shown in the same figure. These are computations which present many technical challenges. We remark later on one way to resolve the issue.

Two sections of this phase diagram have been discussed— the section with $\mu_B = 0$ was discussed in the previous subsection, and the section with $m_s = 0$ was discussed in the section on the $N_f = 2$ phase diagram in T-μ_B-m. Both contain a line of O(4) critical points, and a line of Ising critical points, meeting at a tricritical point. The two lines of O(4) critical points are in fact the same, since they both originate in the finite-T transition for the $N_f = 2$ chiral symmetry restoration. In the 4-dimensional phase diagram one should, therefore, see a single critical surface of O(4) transitions. The boundary of this critical surface is the tricritical line, the two ends of which show up as the two tricritical points we have already discussed. At this tricritical line the O(4) critical surface is glued on to surfaces of Ising criticality. The tricritical line can also be viewed as the boundary of a surface of triple phase coexistence. This much is a direct consequence of the Gibbs phase rule.

The Gibbs phase rule also allows a tetracritical point in a generic four dimensional phase diagram. A tetracritical point is the end point of a line of four-phase coexistence. With a single scalar order parameter, such as $\mathbf{s}$, it is not possible to distinguish four phases. Therefore, we conclude that a tetracritical point should not be seen in the four dimensional phase diagram observed with $\mathbf{s}$.

There remain two generic possibilities for the shape of the phase diagram and they are shown in terms of the corresponding flag diagram in Figure 6. The first possibility is that the tricritical line lies entirely on the side $m_s \geq m_s^{3c}$. The second is that the tricritical line continues to some $m_s^{turn} < m_s^{3c}$ and then bends back towards m_s^{3c}. In the first scenario, the critical line moves to larger m and m_s as μ_B is increased by a small amount from $\mu_B = 0$. In the second, the opposite movement occurs until a large value of μ_B. This is precisely the observation which distinguishes the two lattice studies in [29, 31]. It would be interesting to push lattice studies to smaller cutoffs and decide which scenario is actually obtained in QCD.

In the first case the phase diagram for $m_s > m_s^{3c}$ is qualitatively like the $N_f = 2$ phase diagram, and for $m_s < m_s^{3c}$, similar to $N_f = 3$. In the second case for $m_s^{3c} > m_s > m_s^{turn}$ there are two sheets to the phase diagram at fixed m_s: one similar to the $N_f = 2$ phase diagram, the other like the $N_f = 3$ phase diagram, with the two tricritical points joined by an O(4) critical line, as shown in Figure 7. The inset in the figure shows the unusual phase diagram for fixed non-zero value of m. It would be very interesting if QCD is eventually seen to yield such a phase diagram.

V. CONCLUSIONS

The phase diagram of QCD is complicated. The large global symmetries of QCD imply that there are many thermodynamical intensive parameters, *i. e.*, free parameters which enter the Lagrangian. As a result, there are many different kinds of pairings of quarks that can arise as these parameters are changed. In this paper we have considered only small chemical potentials, defined to be the region where the relevant pairings are between a quark and an antiquark.

The topology of the phase diagram for QCD with two flavours of quarks has been investigated earlier by many authors, mainly in sections of partial symmetry. In this paper we have extended these considerations to the case of physical quark masses, which break both the chiral symmetry and isospin symmetry. Explicit breaking of isospin symmetry by quark masses leads to mixing of isovectors with isoscalars and hence influences the phase diagram (see Section III D 2). This piece of physics is incorporated into the phase diagram that we construct. The topology of this physical phase diagram is strongly constrained by thermodynamics— essentially the Gibbs phase rule (see Section II). Our results are given in Section III E and summarized in the phase diagram shown in (see Figure 4). The physical phase diagram contains a triple line at which phases with and without the chiral and pion condensates coexist. Deducing actual values of the critical and tricritical points in this diagram is a much harder task. However, appropriate Clapeyron-Clausius equations along with the results of current lattice computations [3] place various constraints on them. Improving these constraints through future lattice computations is possible without extreme effort.

The phase diagram of three flavour QCD could be more complicated, since there are even larger global symmetries. Strange quarks can decay into the light quarks through the weak interactions, so one may ask whether this phase diagram is relevant to any physical system. In the context of heavy-ion collisions, where the system is expanding so fast that weak interactions do not come into play in the thermodynamics, strange quarks are indeed relevant.

Further, in the physics of compact stars (involving large chemical potentials), where weak decays of strange quarks are suppressed due to Fermi-blocking of the light quark states into which they could have decayed, strange quarks also become relevant to thermodynamics. Thus the study of the three flavour phase diagram is interesting.

Comparatively little is known at present about this phase diagram. Here we restrict attention to the breaking and restoration of chiral symmetry. The Gibbs phase rule places strong constraints on the topology of the phase diagram. As the strange quark mass is increased keeping the light quarks massless, there is a tricritical value, m_s^{3c}, at which the finite temperature chiral phase transition changes from being first order to second order (for $m_s > m_s^{3c}$). Presently available observations on the lattice [29, 31] can be patched together into two possible phase diagrams which we have discussed in Section IV B. The three-flavour phase diagram can be improved substantially with lattice computations in the near future.

Apart from the results on the QCD phase diagram we believe that this paper demonstrates an useful technique. Usually phase diagrams have been examined by writing down a Ginzburg-Landau theory. As remarked before, these give useful predictions for universal quantities. However, when all symmetries are broken, the usefulness of such a theory is severely curtailed. In such situations, we found that the Gibbs' phase rule is a handy tool for exploring the topology of phase diagrams. When supplemented with the Clapeyron-Clausius equations, it may even be possible to make some quantitative statements of the kind that have been explored in this work.

It is a pleasure to thank Mike Creutz, Saumen Datta, Philippe de Forcrand, Rajiv Gavai, Bengt Petersson, and Misha Stephanov for discussions. This work was supported by the Indian Lattice Gauge Theory Initiative.

---

[1] N. Cabibbo and G. Parisi, *Phys. Lett.*, B 59 (1975) 67;
J. C. Collins and M. J. Perry, *Phys. Rev. Lett.*, 34 (1975) 1353;
A. M. Polyakov, *Phys. Lett.*, B 72 (1977) 477;
L. Susskind, *Phys. Rev.*, D 20 (1979) 2610.

[2] R. D. Pisarski and F. Wilczek, *Phys. Rev.*, D 29 (1984) 338.

[3] Z. Fodor and S. Katz, *J. H. E. P.*, 0203 (2002) 014;
C. R. Allton, *et al.*, *Phys. Rev.*, D 68 (2003) 014507;
Ph. de Forcrand and O. Philipsen, *Nucl. Phys.*, B 642 (2002) 290;
M. D'Elia and M.-P. Lombardo, *Phys. Rev.*, D 67 (2003) 014505;
R. V. Gavai and S. Gupta, *Phys. Rev.*, D 68 (2003) 034506;
R. V. Gavai and S. Gupta, *Phys. Rev.*, D 71 (2005) 114014.

[4] R. F. Dashen, *Phys. Rev.*, 183 (1969) 1245.

[5] J. Gasser and H. Leutwyler, *Nucl. Phys.*, B 250 (1985) 465.

[6] R. G. Edwards *et al.*, *Nucl. Phys. Proc. Suppl.*, 83 (2000) 479;
R. V. Gavai, S. Gupta and R. Lacaze, *Phys. Rev.*, D 65 (2002) 094504.

[7] D. Bailin and A. Love, *Phys. Rep.*, 107 (1984) 325;
M. G. Alford, K. Rajagopal and F. Wilczek, *Phys. Lett.*, B 422 (1998) 247;
R. Rapp *et al.*, *Phys. Rev. Lett.*, 81 (1998) 53.

[8] N. Yamamoto *et al.*, *Phys. Rev.*, D 76 (2007) 074001.

[9] S. Hands, S. Kim and J.-I. Skullerud, *Eur. Phys. J.*, A 31 (2007) 787.

[10] L. McLerran and R. Pisarski, *Nucl. Phys.*, A 796 (2007) 83.

[11] R. B. Griffiths, *Phys. Rev. Lett.*24 (1970) 715.

[12] R. V. Gavai and S. Gupta, *Phys. Rev.*, D 73 (2006) 014004.

[13] M. D'Elia, A. di Giacomo and C. Pica, *Phys. Rev.*, D 72 (2005) 114510.

[14] J. Engels *et al.*, *Phys. Lett.*, B 514 (2001) 299.

[15] F. Karsch and E. Laermann, *Phys. Rev.*, D 50 (1994) 6954;
S. Aoki *et al.*, *Phys. Rev.*, D 57 (1998) 3910;
C. Bernard *et al.*, *Phys. Rev.*, D 61 (2000) 054503;
J. Kogut and D. K. Sinclair, *Phys. Rev.*, D 73 (2006) 074512.

[16] Y. Iwasaki *et al.*, *Phys. Rev. Lett.*, 78 (1997) 179;
A. Ali Khan *et al.*, *Phys. Rev.*, D 63 (2001) 034502.

[17] J. Berges and K. Rajagopal, *Nucl. Phys.*, B 538 (1999) 215;
M. A. Halasz, *et al.*, *Phys. Rev.*, D 58 (1998) 096007.

[18] P. Sorensen (STAR), *PoS* CPOD (2006) 019 [nucl-ex/0701028].

[19] R. V. Gavai and S. Gupta, *Nucl. Phys.*, A 785 (2007) 18.

[20] D. T. Son and M. A. Stephanov, *Phys. Rev. Lett.*, 86 (2001) 592.

[21] J. B. Kogut and D. K. Sinclair, *Phys. Rev.*, D 66 (2002) 034505.

[22] B. Klein, D. Toublan and J. J. M. Verbaarschot, *Phys. Rev.*, D 68 (2003) 014009;
Y. Nishida, *Phys. Rev.*, D 69 (2004) 094501;
A. Barducci, *et al.*, *Phys. Rev.*, D 69 (2004) 096004.

[23] M. Creutz, *PoS*, LAT2005 (2006) 119 [hep-lat/0508012].
[24] R. V. Gavai and S. Gupta, *Phys. Rev.*, D 73 (2006) 014004.
[25] F. Fucito *et al.*, *Phys. Rev.*, D 31 (1985) 1460;
R. V. Gavai *et al.*, *Phys. Rev. Lett.*, 58 (1987) 2519.
[26] F. R. Brown *et al.*, *Phys. Rev. Lett.*, 65 (1990) 2491.
[27] F. Karsch, E. Laermann and C. Schmidt, *Phys. Lett.*, B 520 (2001) 41.
[28] G. Endrődi *et al.*, *PoS*, (LATTICE 2007) 182 [arXiv:0710.0998].
[29] F. Karsch *et al.*, *Nucl. Phys. Proc. Suppl.*, 129 (2004) 614.
[30] T. Herpay and Zs. Szep, *Phys. Rev.*, D 74 (2006) 025008.
[31] Ph. de Forcrand and O. Philipsen, *J. H. E. P.*, 0701 (2007) 077.
[32] The recent claim that a first order transition exists [13] requires further substantiation